Pramana - J. Phys., Vol. 39, No. 6, December 1992, pp. 597–614. © Printed in India.

Inelastic light scattering in strontium borate glasses in the system $xSrO\cdot(1-x)B_2O_3$ and $(SrCl_2)_y\cdot[xSrO\cdot(1-y-x)B_2O_3]_{1-y}$

M H RAHMAN*, B P DWIVEDI, Y KUMAR and B N KHANNA†

Department of Physics, Aligarh Muslim University, Aligarh 202002, India
*On deputation from the Department of Physics, Govt. Edward College, Pabna, Bangladesh

MS received 10 June 1992

Abstract. Raman spectra of strontium borate binary glasses in the system $xSrO\cdot(1-x)B_2O_3$ for $x = 0{\cdot}20$, $0{\cdot}25$, $0{\cdot}30$, $0{\cdot}35$, $0{\cdot}40$, and $0{\cdot}50$ and ternary glasses in the system $(SrCl_2)_y\cdot[xSrO\cdot(1-y-x)B_2O_3]_{1-y}$ for $y = 0{\cdot}10$, $0{\cdot}20$, $0{\cdot}30$ and $0{\cdot}40$ and $x = 0{\cdot}20$ and $0{\cdot}35$, are reported. Raman spectra of the glasses show experimental evidence of glass network modifying nature of SrO in borate matrix. SrO causes a change of boron atom coordination number from 3 to 4 resulting in the complex structural groupings comprising of BO_4 and BO_3 units. Strontium cations are not easily accommodated in the glass structure and tend to break up the network at high concentration (x) of SrO, causing non-bridging oxygens. The effect of temperature variation of binary glasses has also been studied. The introduction of $SrCl_2$ to the binary stronium borate glass causes a large change in intensity of low frequency Raman scattering whereas there is no change in the vibrational dynamics in the high frequency region. The temperature reduced Raman spectra represents true vibrational density of states. Martin–Brenig model developed for the low frequency region has been discussed to obtain the structural correlation range in the glass.

Keywords. Raman spectra; borate glasses; glass structure.

PACS No. 61·40

1. Introduction

For binary borate glasses in the system $xRO\cdot(1-x)B_2O_3$, where R stands for alkali or alkaline earths, Krogh–Moe (1962, 1965) had proposed a model in which borate glasses were described as a random network consisting of boroxol, tri, tetra and diborate etc. structural groups according to specific concentration of RO in v-B_2O_3. Krogh–Moe suggested that this structural model, though based on the experimental observations related to the alkali borate glasses, described as a random network of large borate groups (which are similar to those present in crystalline borate compounds), may also apply to other borate glasses. It is also shown that Raman scattering measurements confirm this model and that typical borate groups exist in borate glasses giving characteristic Raman spectra. This model supported by Konijnendijk (1975) and Griscom (1978), essentially describes the glass former network comprising of B atoms which are partly tri-coordinated and partly tetra-coordinated with O atoms. In general, the units BO_3 and BO_4 are included in larger structural groups whose type and distribution change with changing composition.

†to whom correspondence should be addressed.

We have performed Raman measurements on strontium borate glasses in the systems $x\text{SrO}\cdot(1-x)\text{B}_2\text{O}_3$ and $(\text{SrCl}_2)_y[x\text{SrO}\cdot(1-y-x)\text{B}_2\text{O}_3]_{1-y}$ as functions of x and y of SrO and SrCl_2 respectively and studied the effect of temperature variations. From the earlier investigations on the Raman spectra of borate glasses, it has been evident that a broad depolarized low frequency band (known as boson peak) is observed in most glasses. It is generally believed that this band arises from a breakdown of Raman selection rule (Guha and Walrafen 1984). So knowledge of the density of vibrational states in this region is needed for a better understanding of the reasons due to which this band appears. Shuker and Gammon (1970) showed that the Raman intensity (I) for the Stokes component related to the vibrational density of states (g_b) is,

$$I(w) = C_b[n(w, T) + 1]\, g_b(w)/w \tag{1}$$

where, $n = [\exp(hw/kT) - 1]^{-1}$ is the Bose–Einstein population factor and C_b the coupling coefficient.

We report here the experimental data and calculated vibrational density of states using (1) with presumed values of C_b(i.e., 1, w and w^2) in the low frequency region. Martin–Brenig model (1974) developed for the low frequency Raman scattering in glasses has been used to obtain the structural information about the short correlation range (SCR) in glasses.

2. Experimental

Raman spectra were obtained from the experimental set-up consisting of argon ion laser, a double monochromator with holographic gratings (Jobin Yvon Ramanor U 1000 and HG 2S models) equipped with photoelectric detection to record the Raman signals. The 5145 Å line of the argon ion laser was used as the exciting source with laser power of 860 mW. The spectra were recorded in the conventional 90° scattering geometry. The spectra were also recorded at different temperatures using high temperature unit in the sample compartment equipped with electronic temperature controller.

The binary and ternary glass samples were prepared by heating weighted quantities of strontium carbonate, strontium chloride (Sd Fine Chem, Bombay) and boric acid powder (BDH, Bombay) at 1400 K for one hour in a crucible using an electric furnace. The clear melts were poured into stainless steel moulds kept at 300 K to obtain transparent, homogeneous and colourless glass samples of about 1·5 mm thickness.

3. Raman results

For studying the vibrational dynamics of ternary glasses, we have to first understand the dynamics of the corresponding binary system. Figure 1 shows the spectra of strontium borate glass in the system $x\text{SrO}\cdot(1-x)\text{B}_2\text{O}_3$ at room temperature for $x = 0{\cdot}20$, $0{\cdot}25$, $0{\cdot}30$, $0{\cdot}35$, $0{\cdot}40$ and $0{\cdot}50$. Two spectral regions are important for understanding the results.

(1) The region above 200 cm^{-1}, where two intense bands are centred at 772 cm^{-1}

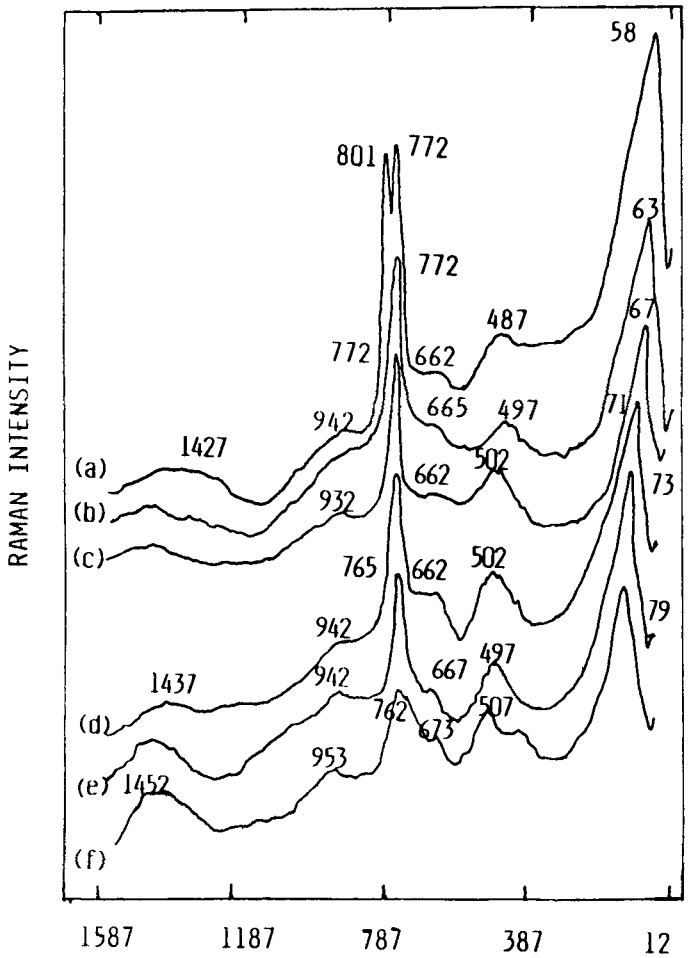

Figure 1. Raman spectra of strontium borate binary glasses in the system $xSrO\cdot(1-x)B_2O_3$ for x; (**a**) 0·20, (**b**) 0·25, (**c**) 0·30, (**d**) 0·35, (**e**) 0·40 and (**f**) 0·50.

and 801 cm^{-1}. (2) The region below 200 cm^{-1}, where a broad band known as boson peak is evident in all the spectra.

3.1 *Chemical mechanism and band assignments*

It is well known from the Raman spectrum of pure v-B_2O_3 glass that an intense and very sharp band at 806 cm^{-1} is the characteristic feature representing planar hexagonal boroxol ring structure (Gallener 1982) of the amorphous glass. The band at 806 cm^{-1} is attributed to the totally symmetric breathing mode of the boroxol ring with very little boron motion involved. Since this mode involves internal oxygen atoms only, it is entirely localized on each ring and thus can account for the extremely small line width ($\sim 16\,cm^{-1}$) observed (Ramos *et al* 1987). The introduction of strontium oxide into the matrix of boric oxide glass causes a break down of some of the boroxol rings, resulting in a change of boron atom coordination number from 3

to 4 and the formation of BO_4 units according to the following scheme (Lorosch *et al* 1984):

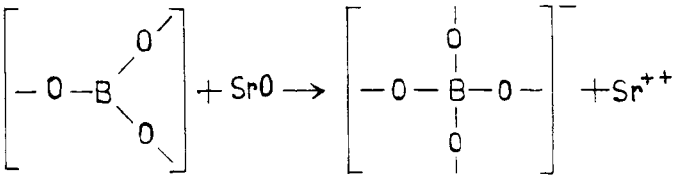

This mechanism liberates strontium cations (Sr^{++}) which increases the ionic conductivity of the glass. The experimental evidence of such a process is the appearance of the Raman band at 772 cm^{-1} with a corresponding decrease in the intensity of the band at 806 cm^{-1} for v-B_2O_3. Figure 1(a) shows a clear splitting of the band at 806 cm^{-1} as a result of addition of xSrO with $x = 0{\cdot}20$ into the v-B_2O_3 matrix, giving rise to a band at 772 cm^{-1} together with the other band at 801 cm^{-1}. The relative intensities of the two bands are nearly equal at the $x = 0{\cdot}20$, but the band at 801 cm^{-1} disappears at $x = 0{\cdot}25$ (figure 1a and 1b). The band at 772 cm^{-1} remains in the same position up to $x = 0{\cdot}30$. The formation of BO_4 groups starts at a concentration $x < 0{\cdot}20$ and reaches the saturation value of glass network coherence at $x = 0{\cdot}25$. This behaviour in strontium borate glasses is different from that of other alkaline earth borate glasses where the formation of BO_4 groups starts at $x < 0{\cdot}20$ but reaches the saturation value of network coherence at $x = 0{\cdot}35$ (Rahman *et al* 1992). These BO_4 units formed by the addition of SrO are incorporated in more complex cyclic edifices, such as tri, penta, di, orthoborate etc. (figure 2). With increasing concentrations (figures 1b–f) of SrO, the intensity of the band at 772 cm^{-1} diminishes and the band position is shifted towards lower wave number. This lowering may be interpreted in terms of the formation of non-bridging oxygens (NBOs) i.e., oxygen atoms not involved in B–O–B linkages (Hosono *et al* 1979 and Nishida *et al* 1980). Table 1 shows the positions of all the observed Raman bands in $x\text{SrO}\cdot(1-x)B_2O_3$ at different values

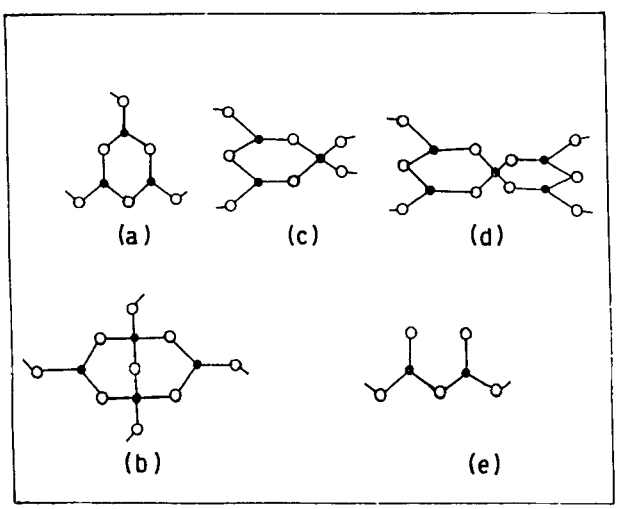

Figure 2. Structural groupings in borate glasses; (**a**) boroxol ring, (**b**) diborate, (**c**) triborate, (**d**) pentaborate and (**e**) pyroborate.

Table 1. Observed position of the Raman bands for strontium borate glasses in the system $xSrO\cdot(1-x)B_2O_3$.

Conc. (x)	Raman bands (cm^{-1})						
0·20	58	487	662	772	801	942	1427
0·25	63	497	665	772	—	939	1462
0·30	67	502	662	772	—	932	1437
0·35	71	502	662	767	—	942	1437
0·40	73	497	667	765	—	942	1427
0·50	79	507	673	762	—	953	1452

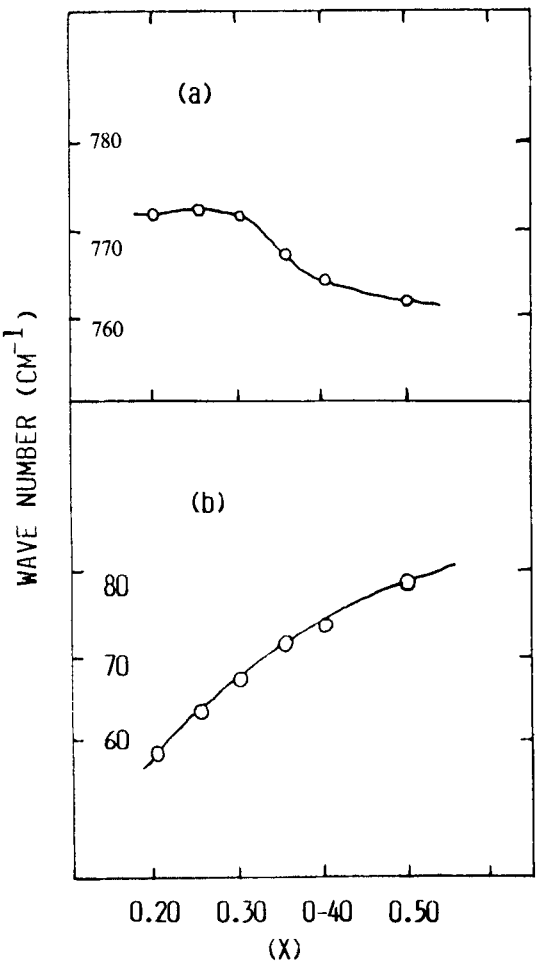

Figure 3. Variation in position of (**a**) 772 cm^{-1} band and (**b**) boson peak with concentration of SrO (x).

of x. The variation in position of 772 cm^{-1} band as a function of concentration (x) is shown in figure 3(a), while the corresponding variation in its peak intensity and half width (FWHM) is shown in figure 4a. At higher concentration (x); i.e., at $x > 0{\cdot}25$, the increase in the number of BO_4 units diminishes and BO_3 groups with NBOs are

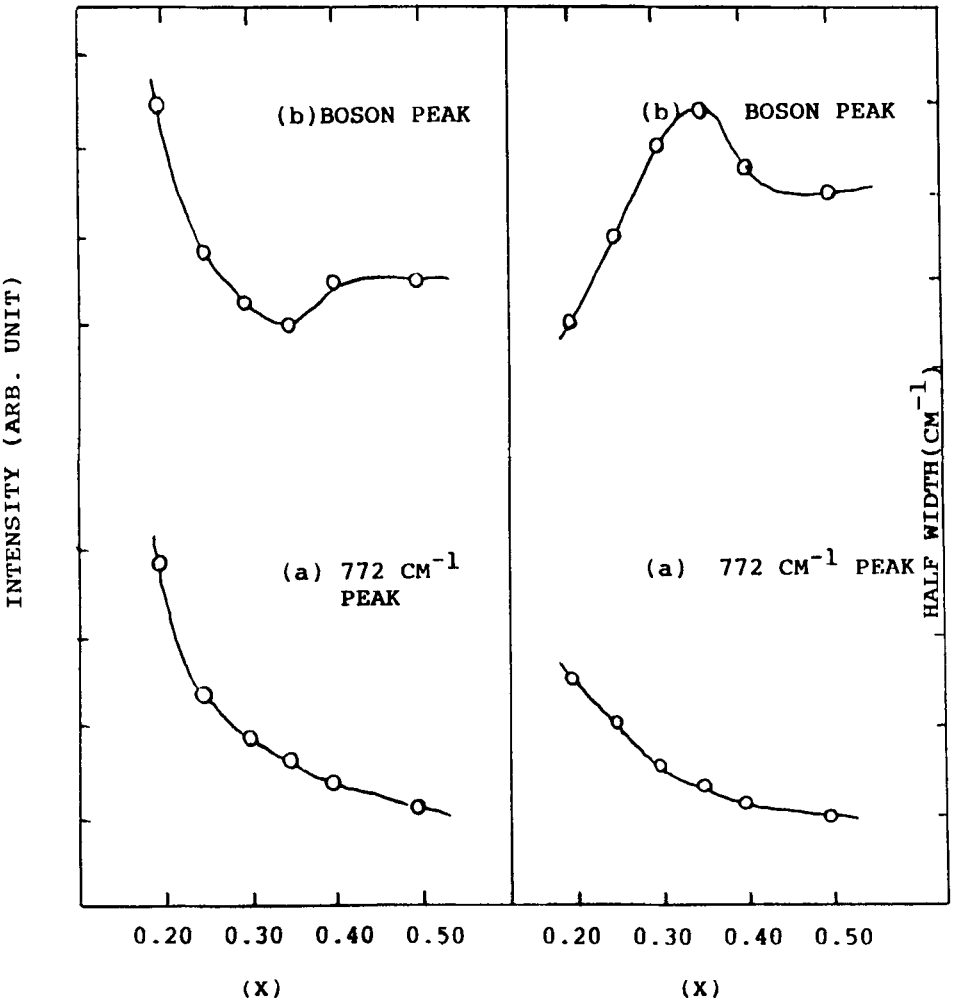

Figure 4. Variation in intensity and half-width (FWHM) for (**a**) 772 cm^{-1} band and (**b**) boson peak with concentration (x).

formed. Large alkaline earth ions are not easily accommodated in the glass structure; they tend to break up the network.

The band at 772 cm^{-1} indicates the formation of six membered borate rings containing one tetrahedral boron and its shift towards lower frequencies at higher concentrations is associated with the formation of six membered borate rings containing two tetrahedrally coordinated borons (Kamitsos *et al* 1987).

The other important feature in the low frequency region of the Raman spectrum is characterized by an unpolarized band known as the boson peak whose position varies from 58 cm^{-1} to 79 cm^{-1} at various composition (x) of the glass (figure 3b). The intensity and half width (FWHM) of the same band at various values of x are shown in figure 4b. This band may arise or be enhanced in intensity due to

(1) an increase in the Bose–Einstein thermal phonon population number, $n(w) = 1/[\exp(hw/kT) - 1]$, where w is the Raman shift; (2) inelastically scattered radiation

which is proportional to $(w_l - w)^4$, where w_l is the frequency of the laser line; (3) Rayleigh wing and also sometimes, Mie or Tyndal scattered stray light; (4) low frequency light scattering from long wavelength acoustic modes of disordered solids and (5) low frequency Raman spectral feature termed as light scattering excess (LSE) attributed to the defect states which are invoked (Anderson *et al* 1972 and Philips *et al* 1972) to describe the amorphous linear temperature-dependent specific heat of glasses at low temperature (Zeller and Pohl 1971; Stephens 1973).

It is a common belief that this low frequency peak is basically due to the thermal population increase with decreasing phonon frequency at room temperature counter-balanced with the decrease in the vibrational density of states. We shall discuss about this peak in greater detail in the later sections. However, according to Almeida (1988), certain Raman active low frequency modes for glasses containing ions of large polarizability probably have major contribution towards the so-called boson peak.

Besides the above mentioned strong features in the spectra of $x\text{SrO}\cdot(1-x)\text{B}_2\text{O}_3$, a broad hump type band is seen in the region 1350–1490 cm^{-1}. This band whose intensity increases with concentration (x) of SrO, is mainly due to different types of boron–oxygen stretching vibrations associated with $>\text{B–O}^-$ groups similar to those observed in $\text{Na}_2\text{O–B}_2\text{O}_3$ glasses (Quan and Adams 1966; Borelli 1963). Such a band is also observed in vitreous and crystalline B_2O_3 spectra around 1450 cm^{-1} (Bratu *et al* 1987). At higher concentration (x) of SrO, this band involves non-bridging oxygens (Kamitsos *et al* 1986) and may be associated with large borate groups with dangling $>\text{B–O}^-$ bonds. At concentration $x = 0{\cdot}50$ the band (figure 1) centring at 1452 cm^{-1} is stronger than the corresponding band observed in the spectra at lower concentrations (x), which indicates that the strontium borate glass of composition $0{\cdot}50\,\text{SrO}\cdot 0{\cdot}50\,\text{B}_2\text{O}_3$ contains cyclic borate groups, i.e., pyro- and orthoborates having dangling $>\text{B–O}^-$ sub groups which are associated with non-bridging oxygens.

Raman bands in the region 900–1100 cm^{-1} appear in borate glasses containing tetrahedral borons (Selvaraj and Rao 1984). So the weak and broad band around 940 cm^{-1} can be attributed to the boron–oxygen stretching of tetrahedrally coordinated borons. Specifically, the band is associated with the group $\{=\text{B–O–B}\equiv\}$ in which one of the borons is tetrahedrally coordinated and the broad band around 1440 cm^{-1} may be attributed to this group (Hogarth and Ahmed 1983). On the other hand some authors (Chryssikos *et al* 1987 and Konijnendijk and Stevels 1977) have attributed this band to the stretch of ortho–borate units since a similar band is observed in the spectra of crystalline alkali and alkaline earth ortho–borates (Konijnendijk 1975).

Bhargava *et al* (1987) observed a weak band around 662 cm^{-1} and assigned it as arising due to the metaborate group. In IR absorption of B_2O_3 glass this band near 656 cm^{-1} is attributed to the bond bending vibration of the B–O–B linkage (Konijnendijk 1975). The band at 470 cm^{-1} in pure B_2O_3 glass has been assigned to the ring bending mode of the boroxol rings (Krogh–Moe 1965). For alkali borate glasses this band is observed at higher wave numbers (Konijnendijk 1975; Konijnendijk and Stevels 1977). For the present system of glasses this band position varies from 487 to 507 cm^{-1} and is probably due to the bending mode of free BO_4 unit or one that is attached very weakly to a ring type structure. From the spectra of figure 1(a–f), it could be seen that this hump type broad band is more or less insensitive to the concentration changes. Minor changes in intensity with concentration are observed in the bands near 662 and 940 cm^{-1}.

In summary, since the crystalline state of the strontium borate sample (in some

composition) shows spectra dissimilar to those of the vitreous state (Konijnendijk 1975), specifically it is difficult to predict the nature of the cyclic groups which could be assigned at the specified composition by means of Raman spectral analysis. However, the presence of cyclic borate groups with non-bridging oxygens, such as pyro-, ortho-borate groups was confirmed from the results of ESR, optical absorption and Mössbauer effect in glasses with high SrO contents (Ohta *et al* 1982).

3.2 *Effect of temperature on binary glass*

Figure 5 shows the spectra of strontium borate binary glasses for $x = 0{\cdot}20$ and $0{\cdot}35$ at different temperatures, while the variations in position and intensity (peak intensity

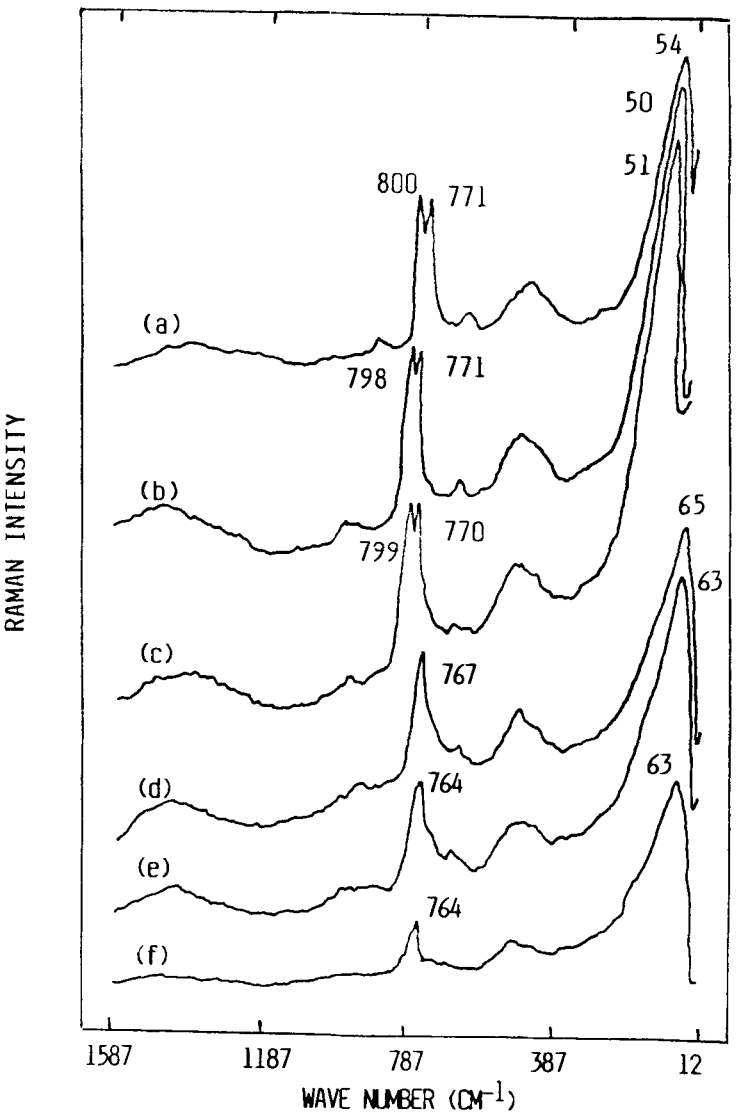

Figure 5. Raman spectra of strontium borate binary glasses in the system $xSrO{\cdot}(1-x)B_2O_3$ for (**a**) $x = 0{\cdot}20$, $T = 373$ K, (**b**) $x = 0{\cdot}20$, $T = 523$ K, (**c**) $x = 0{\cdot}20$, $T = 663$ K, (**d**) $x = 0{\cdot}35$, $T = 373$ K, (**e**) $x = 0{\cdot}35$, $T = 523$ K and (**f**) $x = 0{\cdot}35$, $T = 663$ K.

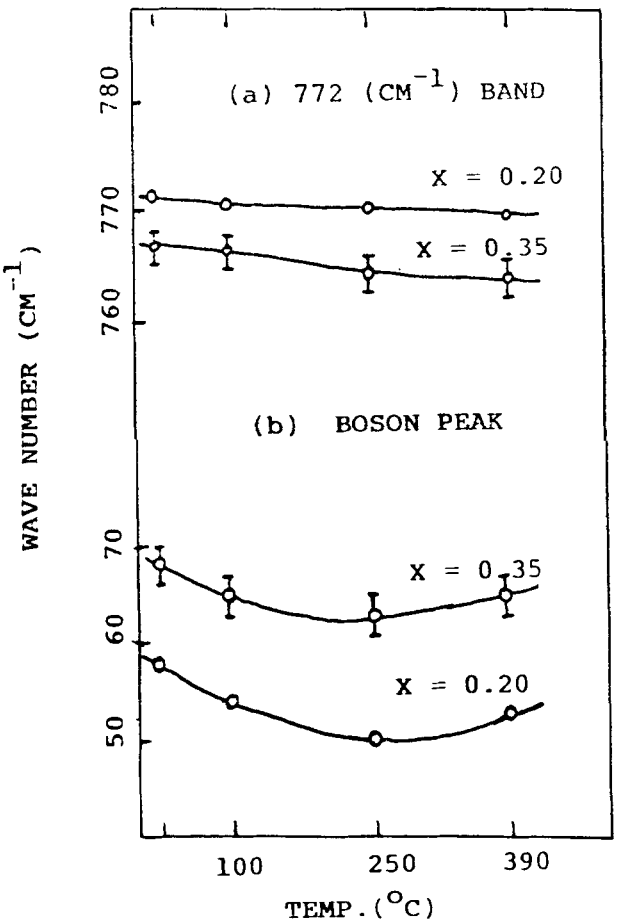

Figure 6. Variation in position of (a) 772 cm^{-1} band and (b) boson peak at different temperatures for $x = 0{\cdot}20$ and $x = 0{\cdot}35$.

and half width (FWHM) for the two important bands i.e., boson peak and 772 cm^{-1} band with temperature at the corresponding concentrations are shown in figures 6 and 7. We see that the position of boson peak shifts towards lower wave number whereas its overall intensity increases appreciably. The other important band at 772 cm^{-1} has minor change in position, but there is a considerable change in intensity and half width (FWHM).

With rising temperature, cyclic borate rings are broken extending the polymeric network of BO_3 triangles, thereby decreasing the density of atoms. So there will be a weakening of the force constants between atoms resulting in a shift of the scattering spectra to lower frequencies. Since the potential wells are closely spaced together, the system would seek a new equilibrium position at different configurational states. The potential minima associated with these states will have different curvatures because of weakening of force constants.

3.3 *Effect of $SrCl_2$ on binary*

The effect of introduction of $SrCl_2$ into the strontium borate binary glasses has been studied in the spectra of the ternary system of glasses $(SrCl_2)_y$ $[xSrO{\cdot}(1-y-x){\cdot}$

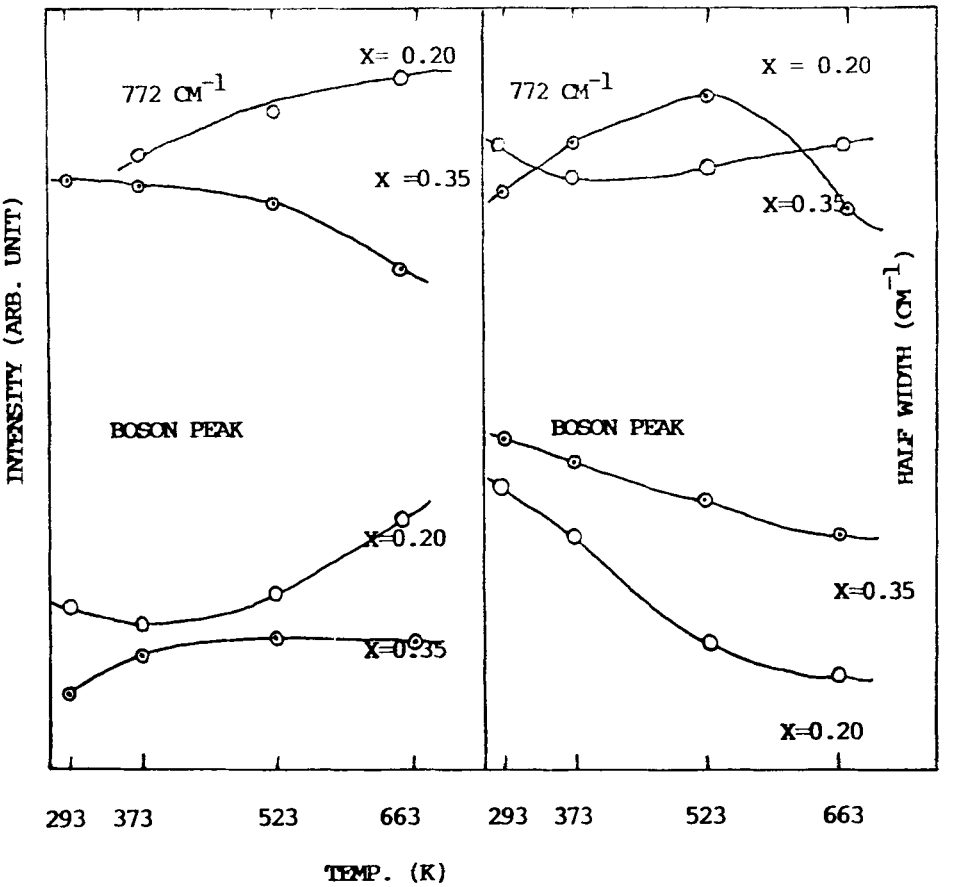

Figure 7. Intensity and half-width variation of 772 cm^{-1} band and boson peak as function of temperature for $x = 0{\cdot}20$ and $x = 0{\cdot}35$.

$B_2O_3]_{(1-y)}$ (figure 8). We see that the presence of $SrCl_2$ in the glass matrix does not substantially modify the vibrational dynamics of the binary glass structure in the region above 300 cm^{-1} (see for comparison figures 1 and 8). We however, observe noticeable modifications in the low frequency region of the spectra due to the addition of $SrCl_2$. The low frequency (<300 cm^{-1}) Raman results are the following:

(1) The overall intensity of the low frequency Raman scattering increases greatly by the addition of $SrCl_2$ into the binary glass (figure 9a).
(2) Boson peak frequency shifts towards higher wave number (figure 9b).
(3) A small shoulder (on boson peak) around 162 cm^{-1} appears and tends to become clear with rise of concentration (y) of $SrCl_2$.

In the later sections we shall be discussing about this low frequency region of ternary glass spectra.

3.4 *Vibrational density of states*

The vibrational density of states $g_b(w)$ can be expressed in terms of reduced Raman spectrum from equation (1) as,

$$g_b(w) = I(\text{obs}) \cdot w / C_b\{n(w, T) + 1\} = I_R. \tag{2}$$

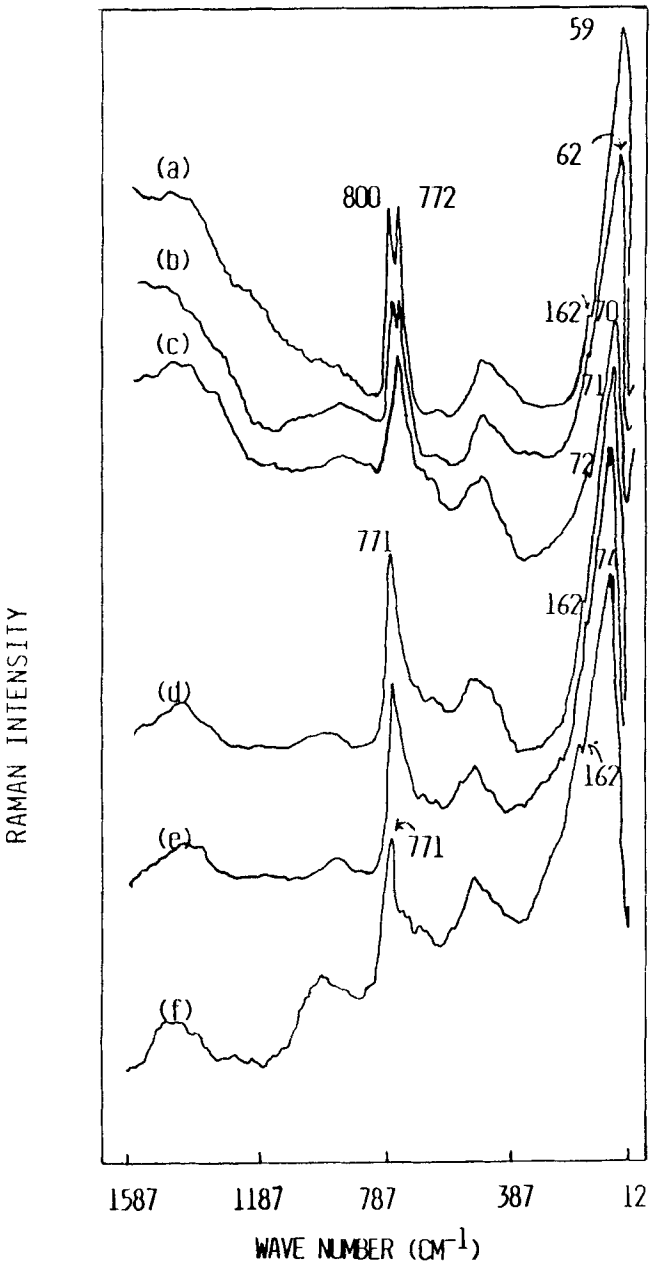

Figure 8. Raman spectra of strontium ternary borate glasses in the system $(SrCl_2)_y \cdot [xSrO \cdot (1-y-x)B_2O_3]_{1-y}$ for various x and y. (**a**) $x = 0{\cdot}20$, $y = 0{\cdot}10$, (**b**) $x = 0{\cdot}20$, $y = 0{\cdot}20$, (**c**) $x = 0{\cdot}35$, $y = 0{\cdot}10$, (**d**) $x = 0{\cdot}35$, $y = 0{\cdot}20$, (**e**) $x = 0{\cdot}35$, $y = 0{\cdot}30$ and (f) $x = 0{\cdot}35$, $y = 0{\cdot}40$.

The reduced Raman intensity I_R is dependent on the coupling coefficient C_b. Arbitrarily, if C_b is assumed to have the values 1, w and w^2, then the frequency reduced Raman spectra ($I_R{}^F$) would be defined as,

$$I_R{}^F(C_b = w^2) = I(\text{obs})/w\{n(w, T) + 1\} \tag{3}$$

and

$$I_R{}^F(C_b = 1) = I(\text{obs}) \cdot w/\{n(w, T) + 1\}. \tag{4}$$

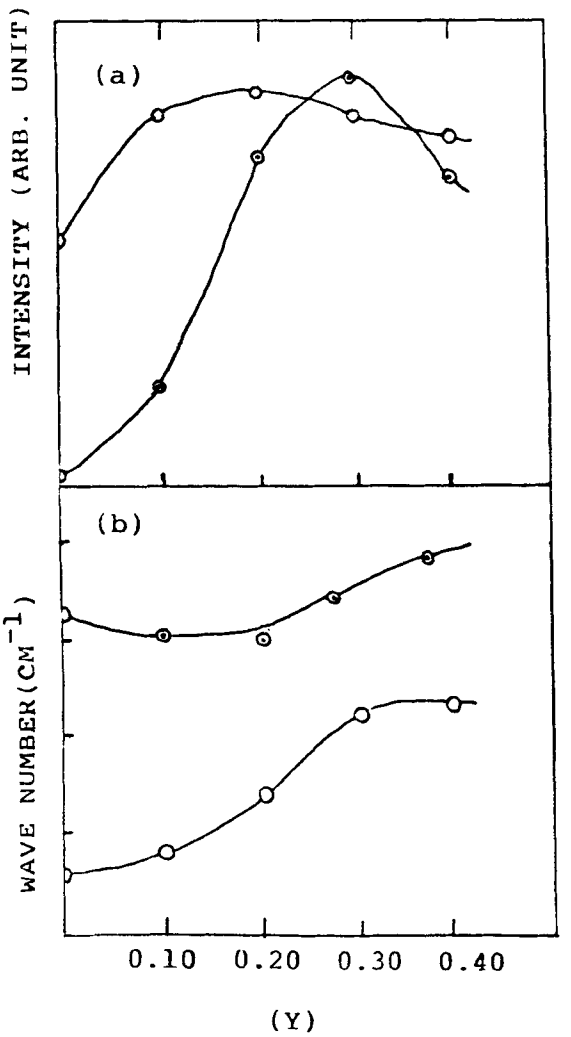

Figure 9. (a) Change in intensity of boson peak with change of concentration y of $SrCl_2$. (b) Shift in frequency of the boson peak with y.

The temperature reduced Raman spectra ($I_R{}^T$) is defined, when $C_b = w$, as,

$$I_R{}^T = I(\text{obs})/\{n(w, T) + 1\} \tag{5}$$

For strontium borate binary glasses, figures 10(a) and (c) show the calculated reduced spectral density of states $I_R{}^F(C_b = w^2)$ and $I_R{}^F(C_b = 1)$ respectively for different concentrations (x). The temperature reduced Raman intensity $I_R{}^T(C_b = w)$ for different concentrations (x) is shown in figure 10(b). We see that in figure 10(a), the spectral shapes and boson peak positions are remarkably similar at all the concentrations (x) to those observed in the experimental raw Raman data in the low frequency region $\langle 300\,\text{cm}^{-1}$ of figure 1. But in the calculated spectral density of states of figures 10(c) and 10(b) for $I_R{}^F(C_b = 1\rangle$ and $I_R{}^T(C_b = w)$ respectively, the spectral shapes are not similar and some shoulder peaks around 75, 140 and $165\,\text{cm}^{-1}$ along with contour maximum (boson peak) are obvious. Also the boson peak position is shifted towards higher wave number.

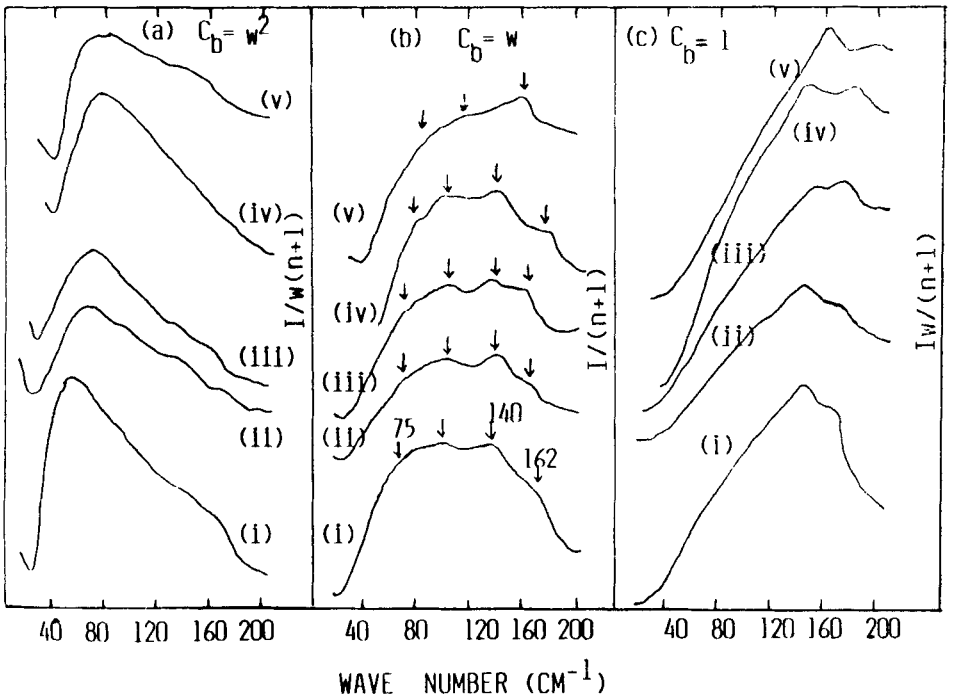

Figure 10. Reduced Raman spectra for (**a**) $I_R^F(C_b = w^2)$, (**b**) $I_R^T(C_b = w)$, (*c*) $I_R^F(C_b = 1)$ in strontium borate binary glasses in the system $x\text{SrO}\cdot(1-x)\text{B}_2\text{O}_3$ for various *x*. (i) 0·20, (ii) 0·30, (iii) 0·35, (iv) 0·40 and (v) 0·50.

The band near 140 cm^{-1} in the temperature reduced spectra is due to librational motion of boroxol rings in $v-B_2O_3$ (Guha and Walrafen 1984). The peak at 75 cm^{-1} for $I_R^T(C_b = w)$ corresponds to the 50 cm^{-1} band in $v-B_2O_3$. These two bands 75 and 140 cm^{-1} have been assigned to in-phase and out-of-phase motions arising from a random distribution of mass and ring size structure (Guha and Walrafen 1984) in $v-B_2O_3$. The addition of SrO to the $v-B_2O_3$ matrix plays an essential role in the formation of tetrahedral BO_4 groups producing borate cyclic units and the introduction of $SrCl_2$ into the binary glass does not affect the vibrational dynamics in the high frequency region. But in the low frequency region there is a large change in boson peak intensity along with the appearance of band at 162 cm^{-1}. For this increase in intensity with increasing $SrCl_2$, two possibilities could be looked into: the addition of $SrCl_2$ helps either in the formation of BO_4 groups, or it takes part in the formation of tetrahedral units, such as BO_3Cl, which may cause the appearance of any band, like the band at 162 cm^{-1}. Though the band around 162 cm^{-1} has not been observed in the experimental raw Raman spectra of strontium binary glass, it arises in the raw spectra of ternary and also in the reduced spectra of binary glasses. Comparing all the spectra of binary and ternary glasses it can be concluded that since the band at 162 cm^{-1} arises in the vibrational density of states for binary, addition of $SrCl_2$ to the binary does not cause the creation of the band; it could only be suggested that addition of $SrCl_2$ enhances the possibility of the appearance of this band and also, as a whole the low frequency band contour intensity increases with rising concentration (*y*) of $SrCl_2$.

3.5 *Boson peak and Martin–Brenig model*

For a disordered system of amorphous materials, where the periodic atomic arrangement inherent in crystalline state lies only within a few coordination spheres, the Raman process is characterized by inelastic light scattering which does not conserve momentum. This shows that the ordered microregion or short correlation range (SCR) in the disordered system leads to a break down of the crystal momentum selection rule (Shuker and Gammon 1970) and the continuous Raman spectra in glasses are ascribed to this disorder-induced scattering. Thus the low frequency light scattering from long wavelength acoustic modes of disordered solids is much important for the low frequency wing of the Raman spectra of glasses.

The theoretical investigation of Shuker and Gammon (1970) shows that the stokes Raman intensity $I(\text{obs})$, reduced by $\{n(w, T) + 1\}/w$, reflects the density of states $g_b(w)$ modulated by the Raman coupling constant C_b. Among the number of experimental procedures proposed (Morgan and Smith 1974; Huttner and Pompe 1982 and Martin and Brenig 1974) for the measurement of the size of ordered microregions or short correlation range (SCR) in glasses, one due to Martin and Brenig (M–B model, 1974) relates the position of boson peak to this coupling coefficient C_b which in turn is related to the structural correlation range (SCR).

The model of Martin and Brenig (1974) applied by Nemanich (1977) to some chalcogenide glasses attributes this low frequency peak to structural disorder of the amorphous material affecting the Raman coupling constant C_b (see equation 1). From (1), assuming $g_b = w^2$ in the Debye-approximation and for solids having electrical and mechanical disorder, the frequency (w) dependence of the Raman coupling constant C_b is expressed, according to the M–B model adapted to right angle scattering geometry (VH configuration) by Nemanich (1977), as

$$C_b(w) = Aw^2[3(v_l/v_t)^5 \exp\{-(2\pi cw)^2\sigma^2/v_l^2\} + 2\exp\{-2\pi cw)^2\sigma^2/v_l^2\}] \quad (6)$$

where, A is a constant, v_l and v_t are the longitudinal and transverse velocity of acoustic waves and 2σ is the structural correlation range (SCR), representing the extent of short range ordering with no damping for phonon propagation in the disordered system. The expression has been derived under the condition that only phonons of wave number w, with

$$(2\pi cw/v_\mu)\sigma < 1, \text{ for } \mu = l \text{ or } t, \quad (7)$$

play a significant role in the scattering. Neglecting the second term in (6) and differentiating with respect to w, one obtains a maximum for C_b at

$$w = w_{\max} = v_t/2\pi c\sigma. \quad (8)$$

We see that the low frequency peak can be attributed to a maximum in the Raman coupling coefficient C_b, which is turn is related to the structural correlation range in glass. From diffraction studies (Mozzi and Warren 1970) SCR in v-B_2O_3 is about 5 Å and the transverse sound velocity in v-B_2O_3 is 1780 m/s (Mazurin *et al* 1985) so that $w_m \sim 19\,\text{cm}^{-1}$. This is in reasonable agreement with the observed values in v-B_2O_3.

In figure 11, typical fits of equation (6) are shown for the binary strontium borate glasses. The experimental points deviate somewhat from the theoretical curves because

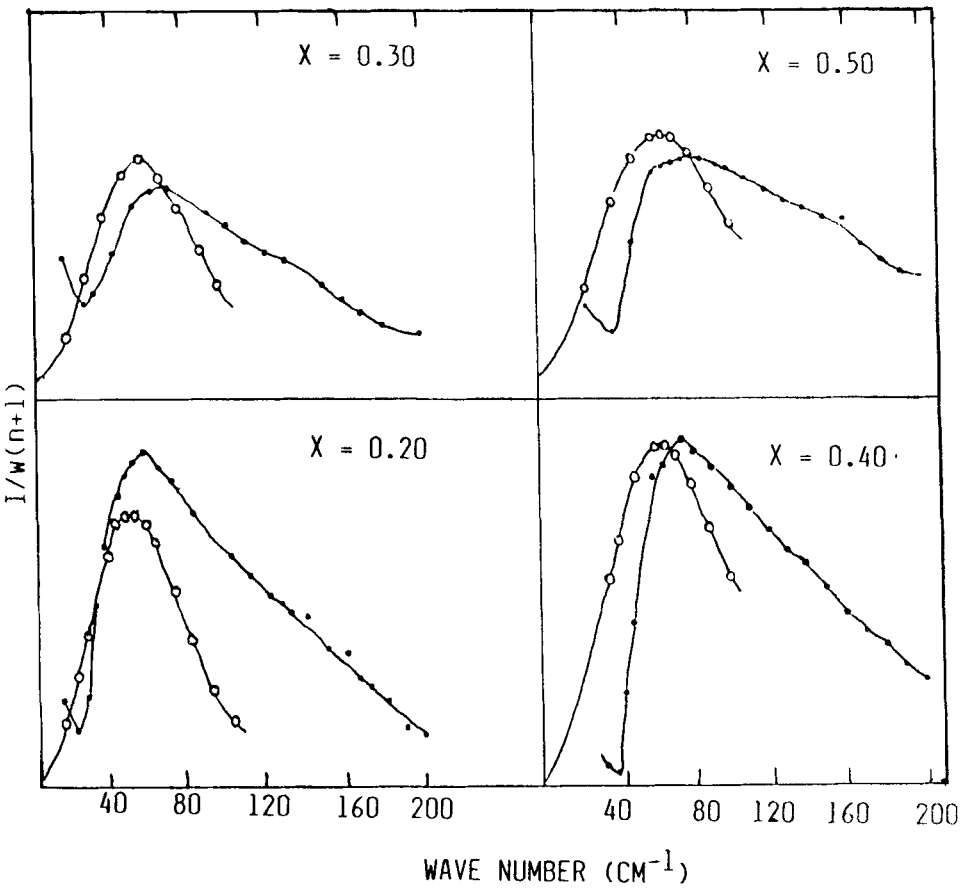

Figure 11. Typical fit of theoretical C_b values of equation (6) with experimental Raman spectra $I_{obs}/w^2(n+1)$ in binary strontium borate glasses for different concentration of SrO (●) experimental (○) theoretical.

of the errors involved in the estimation of the v_l and v_t values which were taken from the reference (Lorosch *et al* 1984). The v_l and v_t values for alkali borate glasses have been shown in figure 12 while the SCR values for binary strontium borate glasses have been shown in table 2.

4. Conclusions

(1) Raman spectral analysis of strontium borate binary glasses in the system $x\text{SrO}\cdot(1-x)\text{B}_2\text{O}_3$ shows the experimental evidence of the glass network modifying nature of SrO in the borate matrix. Addition of SrO to the v-B_2O_3 matrix causes a change of boron atom coordination number from 3 to 4 resulting in the new structural groupings of BO_3 and BO_4 units.

(2) For the glass of composition $25\,\text{SrO}\cdot 75\,\text{B}_2\text{O}_3$ which gives rise to a Raman band at $772\,\text{cm}^{-1}$, network modification becomes saturated in its coherence degree. Tetraborate groups are most probable in this glass. The gradual decrease of band at $772\,\text{cm}^{-1}$ along with its shift indicates that the rate of formation of BO_4 units

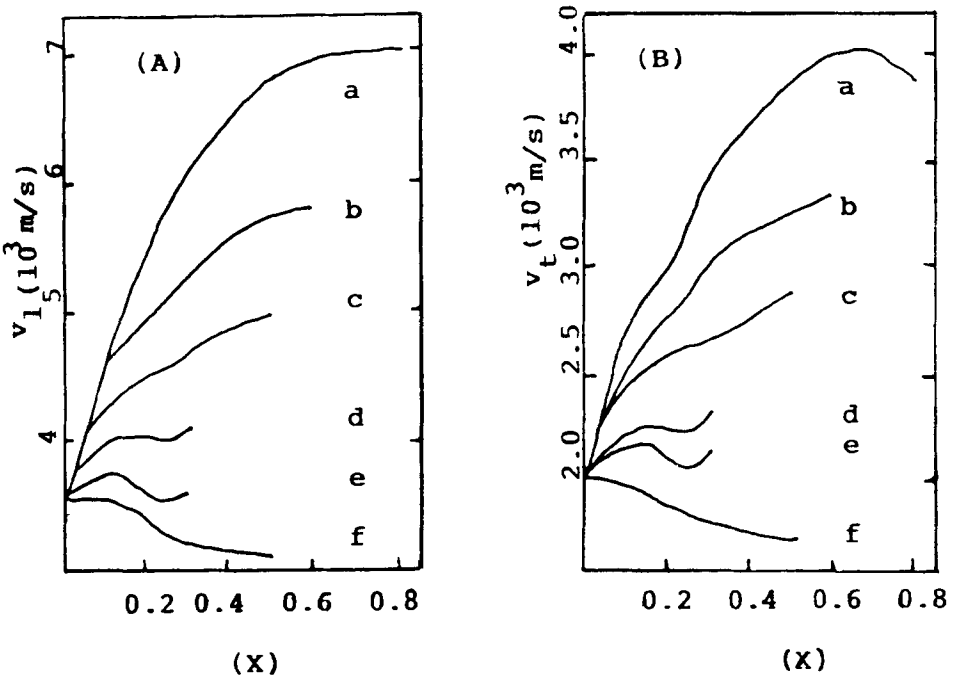

Figure 12. Velocity of longitudinal (A) and transverse (B) acoustic waves in $B_2O_3 - xM_2O$ glasses versus composition (x) for (**a**) Li_2O, (**b**) Na_2O, (**c**) K_2O, (**d**) Rb_2O, (**e**) Cs_2O and (**f**) Tl_2O.

Table 2. The SCR values (2σ) for strontium borate glasses in the system $xSrO{\cdot}(1-x)B_2O_3$.

			2σ(Å)	
x	v_l^* (cm/s)	v_t^* (cm/s)	$v/\pi c\omega$	Curve fitting
0·20	400000	230000	5·7654	5·1665
0·30	405000	229000	5·0226	4·5601
0·35	415000	236000	4·8667	4·5687
0·40	420000	242500	4·8170	4·1375
0·50	430000	250000	4·5687	4·2451

*v_l and v_t values are used from Lorosch *et al* (1984)

diminishes and BO_3 groups (in pyro-, orthoborate) with nonbridging oxygens are formed at high concentrations (x) of SrO. Strontium cations (Sr^{++}) are not easily accommodated in the glass structure and tend to break up the network, causing an increased number of NBOs.

(3) Temperature dependence of binary strontium borate glasses (for $x = 0{\cdot}20$ and $0{\cdot}35$) shows that low frequency boson peak shifts towards lower wave number with rising temperature, but the band at $772\,cm^{-1}$ remains nearly constant in position, with considerable decrease in intensity, which shows an increase of disorder with consequent thermal expansion of the glass.

(4) Addition of SrO to v-B_2O_3 plays an important role in modifying the glass

network, whereas the introduction of $SrCl_2$ into the binary glass causes a large change in intensity in the low frequency region $< 300\,cm^{-1}$ with practically no change in the high frequency region. Raman spectral analysis shows that $SrCl_2$ does not modify the glass structure; only enhances the intensity of Raman scattering in the region $< 300\,cm^{-1}$ (with no drastic change of boson peak position) but some rise of peak position with rise of concentration (y) of $SrCl_2$ shows that the edifice of cyclic borate groups increases which may be due to increased number of strontium cations (Sr^{++}). No change in the high frequency region implies that the ratio of the BO_3 concentrations remains unchanged with rise of $SrCl_2$ concentration. The increase of cations with increase of concentration of $SrCl_2$ increases the ionic conductivity of the strontium borate glasses, similar to the situation observed in alkali borate glasses (Soppe *et al* 1987; Irion *et al* 1980).

(5) Spectral density of states calculated from the reduced Raman data shows that, though frequency reduced Raman spectra ($C_b = w^2$) have the spectral shapes similar to the experimental Raman spectra, the temperature reduced Raman spectra represents true vibrational density of states.

(6) Martin–Brenig model, as discussed in §3·5, provides a useful tool for a direct understanding of the low frequency Raman peak observed in oxide glasses. The low frequency boson peaks are caused by the limited structural correlation lengths in the glass network.

References

Almeida R M 1988 *J. Non-Cryst. Solids* **106** 347

Anderson P W, Halperin B I and Verma C M 1972 *Philos. Mag.* **25** 1

Bratu, Oana P and Monica Culea 1987 *Phys. Status Solidi* **A100** K-195

Bhargava A, Synder R L and Condrate R A 1987 *Mater. Res. Bull.* **22** 1603

Borreli N F 1963 *Phys. Chem. Glasses* **4** 11

Chryssikos G D, Kamitsos E I and Risen W M 1987 *J. Non-Cryst. Solids* **93** 155

Griscom L 1978 in *Borate Glasses* (eds) L D Pye, V D Freschette and N K Kreidl (New York: Plenum) p. 11

Guha S and Walrafen G E 1984 *J. Chem. Phys.* **80** 3807

Gallener F L 1982 *Solid State Commun.* **44** 1037

Hosono H, Kawazoe H and Kanazawa T 1979 *J. Non-Cryst. Solids* **34** 339

Hogarth C A and Ahmed M M 1983 *J. Mater. Sci. Lett.* **2** 649

Huttner B and Pompe W 1982 *Phys. Status Solidi* **B114** 503

Irion M, Couzi M, Levasseur A, Reau J M and Brethous J C 1980 *J. Solid State Chem.* **31** 285

Krogh-Moe 1965 *Phys. Chem. Glasses* **6** 46

Krogh-Moe 1962 *Phys. Chem. Glasses* **3** 101

Konijnendijk W L and Stevels J M 1975 *J. Non-Cryst. Solids* **18** 307

Konijnendijk W L 1975 *Philips Res. Rep. Suppl.* **1** 62

Konijnendijk W L and Stevels J M 1977 *Mater. Sci. Res.* **12** 259

Kamitsos E I, Karakassides M A and Chryssikos G D 1986 *J. Phys. Chem.* **90** 4528

Kamitsos E I, Karakassides M A and Chryssikos G D 1987 *J. Phys. Chem.* **91** 1073

Lorosch J, Couzi M, Pelous J, Vacher R and Levasseur A 1984 *J. Non-Cryst. Solids* **69** 1

Martin A J and Brenig W 1974 *Phys. Status Solidi* **64** 163

Morgan G J and Smith D 1974 *J. Phys.* **C7** 694

Mazurin O V, Streltsina M V and Shvaiko-Shvaikovskaya T P 1985 in *Handbook of glass data, part-B, Single Component and Binary non-silicate oxide glasses* (Amsterdam: Elsevier)

Mozzi R L and Warren B E 1970 *J. Appl. Cryst.* **3** 251

Nemanich R J 1977 *Phys. Rev.* **B16** 1655

Ohta Y, Shimada M and Koizumi M 1982 *J. Non-Cryst. Solids* **51** 161

Philips W A 1972 *J. Low Temp. Phys.* **7** 351

Quan Y T and Adams C E 1966 *J. Phys. Chem.* **70** 331
Ramos M A, Vieira S and Calleja J M 1987 *Solid State Commun.* **64** 455
Rahman M H, Kumar Y and Khanna B N 1992 *Indian J. Pure Appl. Phys.* **30** 327
Shuker R and Gammon R W 1970 *Phys. Rev. Lett.* **25** 222
Stephens R B 1973 *Phys. Rev.* **B8** 2896
Soppe W, Aldenkamp F and Den-Hertog H W 1987 *J. Non-Cryst. Solids* **91** 35
Ulagaraj Selvaraj and Rao K J 1984 *Spectrochim. Acta* **A40** 1081
Zeller R C and Pohl R O 1971 *Phys. Rev.* **B4** 2029